JOURNAL OF CHEMOMETRICS
J. Chemometrics 2003; **17**: 470–479
Published online in Wiley InterScience (www.interscience.wiley.com). DOI: 10.1002/cem.793

Characterizing batch reactions with *in situ* spectroscopic measurements, calorimetry and dynamic modeling

Bei Ma[1], Paul J. Gemperline[1]*, Eric Cash[1], Mary Bosserman[1] and Enric Comas[2]

[1]Department of Chemistry, East Carolina University, Greenville, NC 27858, USA
[2]Rovira i Virgili University, Tarragona, Spain

Received 26 June 2002; Revised 5 November 2002; Accepted 13 December 2002

A method for fully characterizing consecutive batch reactions using self-modeling curve resolution of *in situ* spectroscopic measurements and reaction energy profiles is reported. Simultaneous measurement of reaction temperature, reactor jacket temperature, reactor heater power and UV/visible spectra was made with a laboratory (50 ml capacity) batch reactor equipped with a UV/visible spectrometer and a fiber optic attenuated total reflectance (ATR) probe. Composition profiles and pure component spectra of reactants and products were estimated without the aid of reference measurements or standards from the *in situ* UV/visible spectra using non-negative alternating least squares (ALS), a type of self-modeling curve resolution (SMCR). Multiway SMCR analysis of consecutive batches permitted standardless comparisons of consecutive batches to determine which batch produced more or less product and which batch proceeded faster or slower. Dynamic modeling of batch energy profiles permitted mathematical resolution of the reaction dose heat and reaction heat. Kinetic fitting of the *in situ* reaction spectra was used to determine reaction rate constants. These three complementary approaches permitted simple and rapid characterization of the reaction's rate of reaction, energy balance and mass balance. Copyright © 2003 John Wiley & Sons, Ltd.

KEYWORDS: multivariate curve resolution; self-modeling curve resolution; multiway analysis; process analysis; batch process analysis; calorimetry; UV spectroscopy; kinetic fitting

1. INTRODUCTION

In the chemical and pharmaceutical industries there is a great need to improve the effectiveness of batch operations [1,2] by optimizing process conditions to improve safety [3] and yields [4] and reduce waste. Classical off-line analysis methods such as GC/MS and HPLC have many associated problems in batch process analysis applications, such as sample processing, sample handling and instrument maintenance, that affect system stability and reproducibility. Quenching the reaction during sample preparation destroys reactive intermediates, so the composition of the sample analyzed does not accurately reflect the composition of the reaction mixture [5]. The time consumed by these methods is also a serious drawback. The ease with which *in situ* spectroscopic measurements can be made when coupling the spectrometer with fiber optics makes process spectroscopy a much more effective choice over chromatography for process analysis. Spectroscopic measurements have great potential in 'on-line' process analysis, because under the right conditions they can be used as a truly non-invasive monitoring technique. Chemometric tools, in principle, are particularly well suited for improving the effectiveness of process analytical techniques through two main functions: (1) extracting a wealth of useful information from convoluted measurements and (2) facilitating the automation of *in situ* analytical techniques. UV/visible spectroscopy is somewhat less common than infrared (IR) or near-infrared (NIR) in process applications, but has a unique combination of advantages: (1) the UV/visible region has high sensitivity regardless of its broad and less informative spectra; (2) unlike IR and NIR, water does not absorb between 200 and 750 nm, so interference from water is not present; (3) optical fibers for use in the UV/visible region are readily available; and (4) attenuated total reflectance (ATR) UV/visible spectroscopy can be used in very opaque liquid samples.

*Correspondence to: P. J. Gemperline, Department of Chemistry, East Carolina University, Greenville, NC 27858, USA.
E-mail: gemperlinep@mail.ecu.edu
Contract/grant sponsor: National Science Foundation; Contract/grant number: CHE-0201014.
Contract/grant sponsor: Measurement and Control Engineering Center (MCEC).

Copyright © 2003 John Wiley & Sons, Ltd.

1.1. Self-modeling curve resolution (SMCR) method

Self-modeling curve resolution (SMCR) [6] describes a class of chemometric tools for estimating pure component spectra and composition profiles from mixture spectra. Under the assumption that pure component profiles and spectra should be non-negative and composition profiles should be unimodal, mathematical solutions are produced [7–9]. In many cases, SMCR may be the only method available for resolving the composition profiles and pure component spectra from *in situ* spectroscopic measurements [5]. Unlike multivariate calibration techniques, no reference measurements are required and prior knowledge of the number and nature of the chemical species in the mixture is not needed. In this paper a multiway SMCR method based on non-negative ALS [9,10] was used to analyze mixture spectra measured from consecutive batch reactions. Consecutive batches were analyzed simultaneously by unfolding the multiway matrix along the time axis. By comparing the SMCR results from multiple batches, the following two questions were answered. Which batch produced more or less product? Which batch produced the product faster or slower?

Reaction spectra, measured as a function of time, can be represented as rows in a matrix **D**. According to Beer's law, **D** can be expressed as a product of k vectors representing concentration profiles and k vectors representing the spectra of the pure components, i.e.

$$\mathbf{D} = b\mathbf{CP} \tag{1}$$

where **D** is a data matrix with i absorption spectra of mixtures in each row measured at j wavelengths, b is the path length, which remains constant throughout the experiment, **C** is a data matrix with each column representing the concentration profile of each pure component, and **P** is a matrix with each row containing the absorption spectrum of each pure component.

The resolution of data matrix **D** into pure component profiles and concentration profiles can be achieved via a constrained least squares procedure [10] by alternately applying Equations (2) and (3) until convergence is reached subject to the constraints in Equation (4):

$$\mathbf{P} = \mathbf{C}^{+}\,\mathbf{D} \tag{2}$$

$$\mathbf{C} = \mathbf{D}\mathbf{P}^{+} \tag{3}$$

$$\mathbf{P} \geqslant 0 \quad \text{and} \quad \mathbf{D}\mathbf{P}^{+} \geqslant 0 \tag{4}$$

where the superscript '+' indicates the pseudoinverse of a matrix. The iterative optimization starts with the evaluation of the unknown spectra using Equation (2) and an initial estimate of **C** from the needle search technique [11] or evolving factor analysis [12]. In the next step the concentration matrix **C** is updated using Equation (3). These steps are repeated until convergence is achieved. In most cases, non-negativity constraints must be applied to concentration profiles and component spectra to achieve reasonable solutions [13].

When multiple batches are used, K data matrices are obtained under various initial conditions (e.g. different starting concentrations of the chemical constituents), producing a set of data matrices $\mathbf{D}_k$:

$$\mathbf{D}_k = \mathbf{C}_k\mathbf{P}, \qquad k = 1, 2, \ldots, K \tag{5}$$

where $\mathbf{C}_k$ is the matrix of concentration profiles of the chemical species spectroscopically active in $\mathbf{D}_k$, and **P** is the matrix of the unit pure spectra of these species. The concatenated data matrix **D** is obtained by arranging each of the data matrices $\mathbf{D}_k$ in consecutive order, with the columns (wavelengths) in common and with a number of rows equal to the total number of acquired experimental spectra in the different data matrices $\mathbf{D}_k$ [14]. As a first step the initial estimate of the concatenated matrix of the concentration profiles, **C**, is built up from the initial estimation of the submatrices $\mathbf{C}_1,\ \mathbf{C}_2, \ldots,\ \mathbf{C}_k$ obtained by SMCR of the submatrices $\mathbf{D}_1,\ \mathbf{D}_2, \ldots,\ \mathbf{D}_k$. At each iteration the new estimates of the matrix of spectra, **P**, and the matrix of concentration profiles, **C**, are obtained [13]. There may be two kinds of deviations from the ideal multiway SMCR model described by Equation (5), i.e. batch-to-batch differences and within batch differences.

In multiway analysis the pure component spectra of the common species are assumed to be the same in all batches. This assumption may be true only when the physical conditions such as temperature and solvent composition are kept constant. However, it is frequently possible and sometimes even desirable to have different conditions from batch to batch. For example, the temperature might change over time, and under conditions typically used in industry, there is usually a large change in the reaction mixture composition over time. All these factors can affect the shape of pure component spectra. In order to find the best process conditions, large differences in temperature, concentration and solvent are introduced according to the principles of experimental design when optimizing a batch process. The variations in the spectral profiles from batch to batch can cause difficulty in multiway analysis and make the SMCR results incompatible with each other. Within batch differences, e.g. due to unwanted temperature gradients during the batch, can also be problematic. In this particular study, between-batch variations in spectral profiles were found to be a more important problem than within-batch differences.

A variation of multiway SMCR was developed using non-negative ALS steps to alleviate these problems. The first step of the method is to apply SMCR to each batch separately to produce initial estimates of concentration profiles and pure component spectra. Next the mean value of the pure component spectra estimated from all batches, $\overline{\mathbf{P}}$, is calculated so that the spectral profiles can be kept as similar as possible. Then an ALS optimization step is used to minimize the spectral differences subject to non-negativity constraints. For a given $\overline{\mathbf{P}}$ a suitable $\mathbf{P}_{\text{new}}$ is found for each batch measurement, which minimizes the difference between $\overline{\mathbf{P}}$ and $\mathbf{P}_{\text{new}}$ as shown in Equation (6) subject to the non-negativity constraints for each individual $\mathbf{D}_k$ as shown in Equation (7):

$$\min \|\overline{\mathbf{P}} - \mathbf{P}_{\text{new}}\| \tag{6}$$

$$\mathbf{P}_{\text{new}} \geqslant 0 \quad \text{and} \quad \mathbf{D}_k\mathbf{P}_{\text{new}}^{+} \geqslant 0 \tag{7}$$

Copyright © 2003 John Wiley & Sons, Ltd.

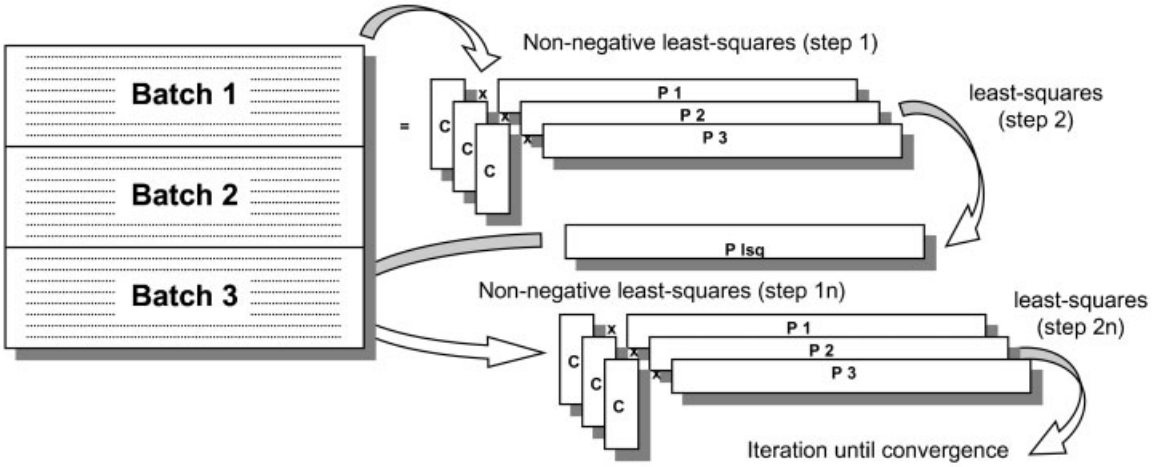

Figure 1. Illustration of the modified multiway analysis algorithm.

where $\overline{\mathbf{P}}$ is the data matrix of mean spectra from the initial SMCR analysis of the selected measurements and $\mathbf{P}_{\text{new}}^{+}$ is the pseudoinverse of the data matrix $\mathbf{P}_{\text{new}}$. Once all K data sets are fitted, a new mean is calculated and used in Equation (6). This iterative procedure is repeated until $\mathbf{P}$ reaches convergence or the maximum iteration number is reached. Figure 1 is a graphic illustration of the modified multiway analysis procedure. By using the multiway SMCR method with alternating least squares optimization steps, the maximum similarity of spectra between batches is maintained while allowing small variations in the estimated pure component spectra from batch to batch.

1.2. Reaction calorimetry method and techniques

Reaction calorimetry has found widespread acceptance as a valuable tool for evaluation of thermal hazards for batch-type reactors [15]. Exothermic chemical reactions in the fine chemical and pharmaceutical industries are commonly carried out in multipurpose batch reactors and can be conveniently studied in laboratory 'reaction calorimeters' [16]. These devices are based upon conventional jacketed laboratory reactors, from 50 ml to 1 l in volume, and can provide valuable information about the safety and operability of processes. Reaction calorimetry allows the heat output rate Q_r for a reaction to be determined from a heat balance over the reactor:

$$Q_r = Q_{rem} + Q_L + Q_{accum} + Q_{dose} \tag{8}$$

where Q_L is the heat loss from the vessel, Q_{rem} is the heat removed (or added) by the oil circulating around the vessel jacket, Q_{accum} is the heat (if any) accumulated by the reactant and reactor and Q_{dose} is the heat taken up by the feed (if any). Most of the terms can be inferred from measurements carried out on the reactor. In power-compensated isothermal heat flow calorimetry [17] the controlled variables are the reactor jacket temperature and reactor heater power. The measured variable is the reactor–jacket temperature difference. The relationship between this quantity and heat flow from the reactor can be described by

$$Q = UA\,\Delta T \tag{9}$$

where U is the heat transfer coefficient from the reaction mixture to the reactor wall, A is the wet area of the cold reactor wall in contact with the reaction mixture and ΔT is the reactor–jacket temperature difference.

In the power compensation calorimetry experiment the oil circulator is arranged to be at a fixed temperature below the reactor set point. Electrical heat Q is supplied to the system from the power compensation heater to maintain the required reactor temperature. A controller maintains a constant temperature difference ΔT between the oil circulator and the reaction mixture. Figure 2 illustrates the power compensation calorimetry method.

Before the reaction starts, the power needed to maintain a constant temperature difference between the reactor and the jacket is measured and $Q = UA\ \Delta T$ is estimated. As heat is liberated (exothermic) or absorbed (endothermic) during a chemical reaction, the controller adjusts the electrical power to the heater to maintain isothermal conditions. The change in power during a chemical reaction forms the basis of the calorimetric analysis. The heat of the reaction can be determined by measuring the change in power relative to the steady value before the reaction.

Applying a heat balance equation to the reactor throughout the period of the reaction gives the expression

$$Q_r = Q_{elec} + Q_{rem} + Q_L + Q_{accum} + Q_{dose} \tag{10}$$

where Q_r is the power output of the reaction, Q_{elec} is the power input by the power compensation heater, Q_{rem} is the power removed from the reactor by the cooling jacket, Q_L is the power loss from the reactor through other sources, e.g. convection and radiation, Q_{dose} reflects the heat released or absorbed by the feed material dosed into the reactor and Q_{accum} is the power accumulated in the reactor, which is always zero in isothermal operation. Addition of reagents changes the heat transferred to the jacket, $Q = UA\ \Delta T$, by increasing A, the wet surface area of the jacket in contact with the reaction mixture, and by changing U, the thermal conductivity of the system. After the reaction is complete and constant-temperature conditions are once again achieved, the power needed to maintain isothermal conditions is measured and the new $Q = UA\ \Delta T$ is estimated. Knowing the time and rate at which reagent is introduced and

Copyright © 2003 John Wiley & Sons, Ltd.

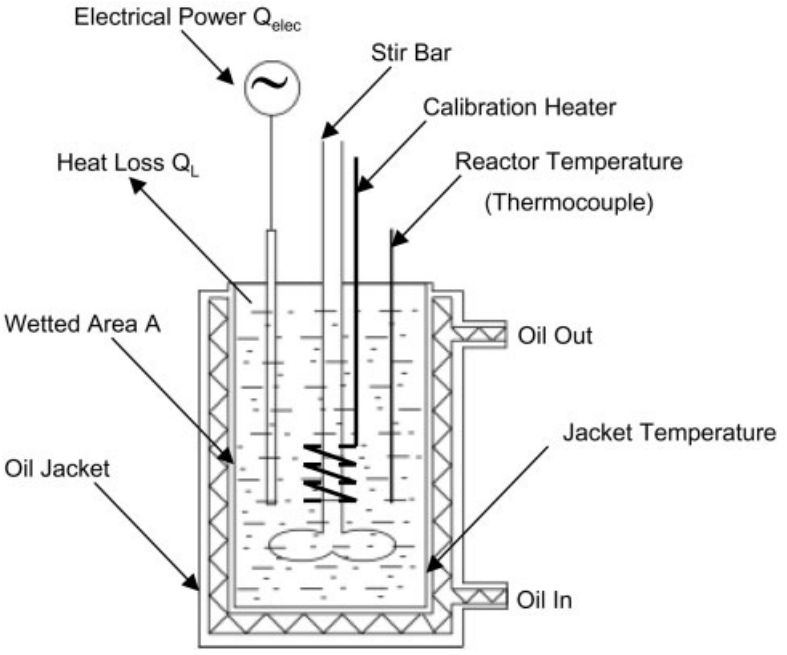

Figure 2. Schematic diagram of the reaction calorimeter.

assuming that the change in U is negligible, the increase in A as a function of time is estimated by interpolation.

2. EXPERIMENTAL

2.1. Equipment

The Auto-MATE reactor system (Hazard Evaluation Laboratory Limited (HEL Ltd), Hertfordshire, UK) is a miniature ($\sim$50 ml) computer-controlled multiple-reactor system. Process conditions, including reaction temperature, jacket temperature, reagent feed and agitation, were controlled by WinISO® software from HEL Ltd running on a 500 MHz Pentium III computer. The auto-MATE mini reactor system was modified to accept fiber optic attenuated total reflectance (ATR) UV/visible probes from Equitech International (Aiken, SC, USA).

A four-channel fiber optic CCD UV/visible spectrometer from Equitech International was used to measure UV/visible spectra and consisted of a Millennium 3 (M3) UV/visible spectrograph with a 1024×512-element thermoelectrically cooled CCD array and an Xe flash lamp. The spectrograph was designed for simultaneous imaging of 400 μm core input fibers over a wavelength range of 190–790 nm. The ATR probe was a three-bounce design with a 10 mm hemispherical sapphire crystal housed in a stainless steel probe 12.5 mm in diameter $\times$ 100 mm long, having an effective total path length of approximately 1.5 μm. Sapphire allowed response down to 220 nm in samples with an index of refraction of up to 1.5 and offered excellent resistance to chemical attack. Each probe had two 400 μm core fused silica fibers spaced oppsite each other in a semicircle around the circumference of the ATR hemisphere crystal. Both fibers emerge from the rear of the probe in a single tube of stainless steel armor.

Spectrometer data acquisition was performed using the software package IntelliFORM® (H&A Scientific, Greenville, NC, USA) running on the same computer used for control and operation of the reactor. IntelliFORM was used to adjust the CCD integration time, flash lamp duration and number of pulses so that the intensity of light falling on the CCD matched the fiber optic probe light throughput characteristics, ensuring optimum use of the CCD and A/D converter dynamic range with a maximum digitized intensity in the range of 6.5×10^4 counts. IntelliFORM was used to process the CCD images to extract wavelength-calibrated absorbance spectra from all four fiber channels simultaneously. IntelliFORM includes self-modeling curve resolution (SMCR) software to estimate composition profiles of reactants, intermediates and products for single as well as multiple batches.

2.2. Reaction conditions

The reaction used to study the capabilities of the combined calorimeter–UV/visible spectrograph and multibatch SMCR software was the acetylation of salicylic acid by acetic anhydride with phosphoric acid as catalyst. A 2.5 ml volume of *o*-phosphoric acid (Fisher Scientific, Fair lawn, NJ, USA) was added to a 500 ml container of acetic anhydride (Fisher Scientific) and mixed completely. Then 30 ml of this mixture was used as the initial reactor charge in the 50 ml reactor vessel, and the reactor system was equilibrated for 40 min at the desired reaction temperature. Accurately weighted aliquots of salicylic acid in the range of 7–10 g (Fisher Scientific) were dosed into the glass reactor vessel over a time interval of about 30–60 s after the 40 min equilibration time. The reagents were allowed to react for 60–90 min. The reactor jacket temperature was held constant with an oil circulator system at 45, 55 or 65°C. The reactor temperature was held 10°C higher than the jacket temperature by the autoMATE electrical heater, controller and WinISO control software in the power compensation calorimetry mode of operation. The reaction conditions were varied to produce different amounts

Copyright © 2003 John Wiley & Sons, Ltd.

Table I. Factorial design for batch acetylation of salicylic acid

Batch	Temp. (°C)	Amount of acetic anhydride (mol)	Amount of salicylic acid (mol)
I	65	0.3141	0.0628
II	55	0.3141	0.0785
III	75	0.3141	0.0785
IV	55	0.3141	0.0524
V	75	0.3141	0.0524

of product at different reaction temperatures according to the two-factor experimental design shown in Table I.

Spectra of the reaction mixture were recorded at 30 s intervals during the reaction for a period of 60–90 min. Parameters for spectrometer operating conditions include the number of flash lamp triggers (usually in the range of 3–5), number of exposures (10), trigger width (250), trigger period (3), auxiliary gain (1) and time delay (0.1 s).

3. RESULTS AND DISCUSSION

3.1. Multiway SMCR results

The wavelength region used for multiway self-modeling curve resolution analysis was from 280 to 390 nm (see Figure 3). Non-linear detector response was observed in the UV region below 280 nm owing to a total absorption above 1.0 where the measurements tend to be affected by stray light. The bottom trace shows the starting spectrum of acetic anhydride, which does not absorb light in the selected wavelength region. The top traces show how the reaction spectra change after the addition of salicylic acid. The spectral region from 376 to 390 nm was used for baseline correction, since the reagents had no absorption in that region. Overlay plots of spectra from different batches showed small shifts ($\sim$2–5 nm) in the position of absorption maxima. It was presumed that these small shifts were the result of large temperature differences and large concentration differences from batch to batch.

A strong and unique UV/visible absorbance peak for salicylic acid can be observed in the region from 290 to 360 nm. The absorbance of this peak decreased as a function of time, corresponding to the consumption of salicylic acid. The smaller and narrower absorption band at about 285 nm increased as a function of time and is associated with the production of acetylsalicylic acid. The spectrum labeled 'Start' marks the starting point of the reaction, which shows the maximum concentration of salicylic acid in the solution. The spectrum labeled 'Finish' marks the ending point of the reaction, which shows the maximum concentration of product in the solution of excess acetic anhydride and acetic acid.

Figure 4 shows the estimated composition profiles resulting from the multiway self-modeling curve resolution analysis of five consecutive batches under conditions of different temperature and different amount of initial reactant charge. Despite the fact that there were small shifts in the position of absorption maximum over the different batches, the multiway SMCR method performed well, capturing 99.98%–99.99% of the sum of squares. The SMCR-estimated composition profiles are plotted in overlay fashion in Figure 4A and are plotted serially in Figure 4B.

Pure component spectra for the two components estimated by multiway SMCR varied slightly from batch to batch. The average spectra are shown in Figure 5 with error bars drawn at ± 2 standard deviations to show the variation from batch to batch. One possible source of spectral variation could be differences in the index of refraction of the reaction medium from batch to batch caused by different concentrations and operating temperatures. A large difference in the index of refraction between the ATR probe crystal and the reaction medium will help minimize spectral variation due to changes in the index of refraction in the reaction medium, however, in these experiments a sapphire ATR crystal was used in the fiber optic probe which has only a small difference from the index of refraction of the reaction medium. Therefore it seems reasonable to conclude that these spectral measurements might exhibit small concentration- or temperature-induced batch-to-batch variations.

The multiway SMCR approach used here permits small variations in the pure component spectra from batch to batch while solving batch-to-batch scaling ambiguities in the reaction profiles. One-at-a-time SMCR analysis would also permit variations in the spectra from batch to batch but would not resolve scale ambiguities in the concentration profiles,

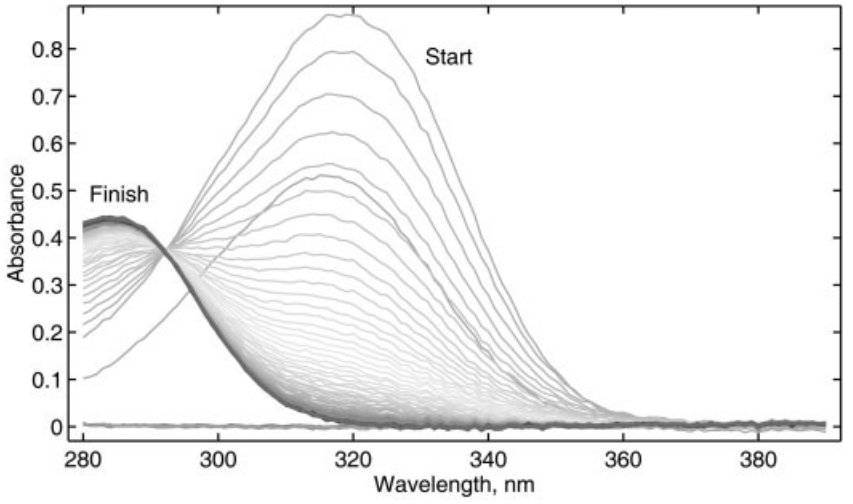

Figure 3. Batch I UV/visible spectra at 65°C with 8.6806 g of salicylic acid.

Copyright © 2003 John Wiley & Sons, Ltd.

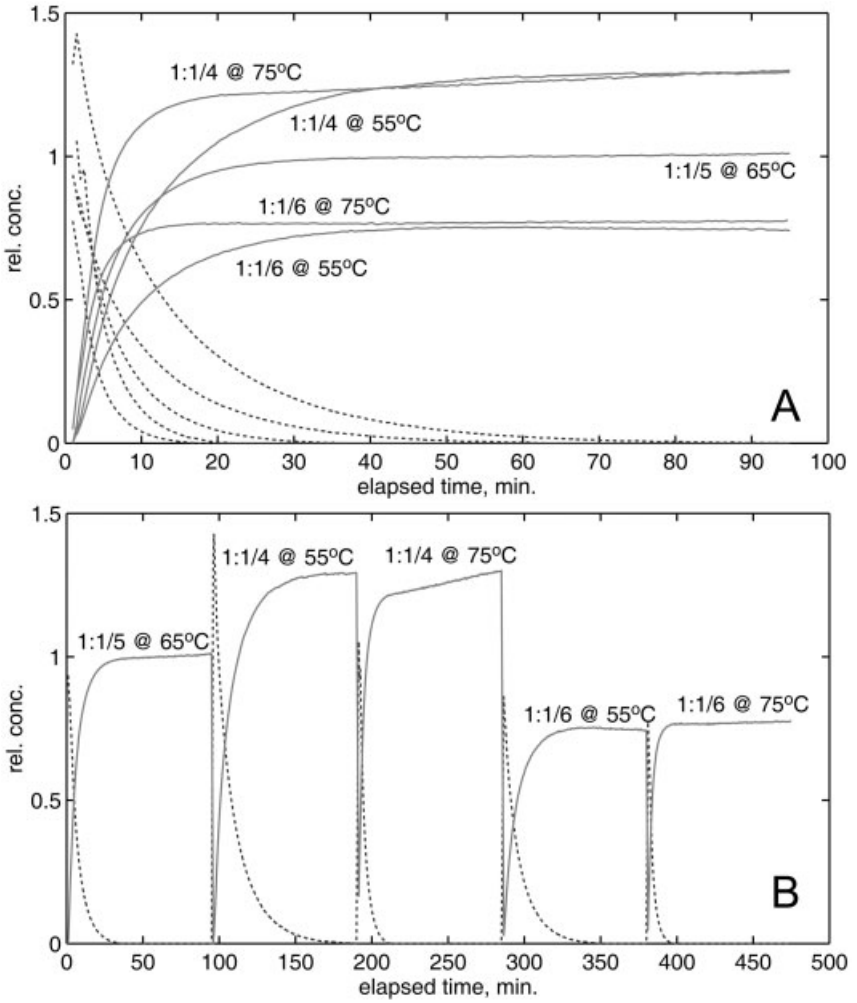

Figure 4. Estimated composition profiles from multiway SMCR. Overlay plot (A) and serial plot (B) of reaction profiles from all five batches. Reactant: broken lines. Product: full lines.

making it impossible to answer the question 'Which batch made more or less product?'. The conventional multiway ALS approach did not allow small deviations in the spectra from batch to batch which gave perturbations in the resolved concentration profiles (not shown).

The SMCR product profiles show that the final amount of product formed in each batch is consistent with the amount of product expected (see Table II). The SMCR concentration profiles clearly show which batches formed more product or less product and which batches reacted faster or slower.

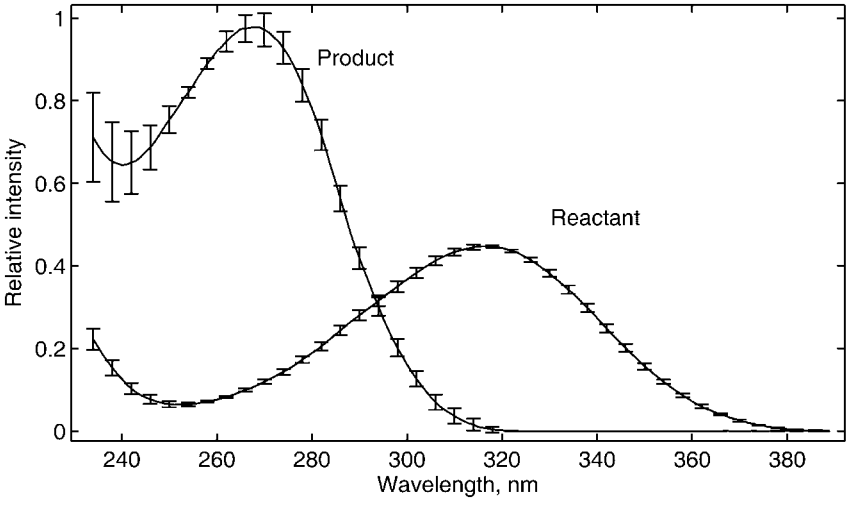

Figure 5. Estimated pure component spectra from multiway SMCR. Error bars show batch-to-batch variation at ± 2 standard deviations.

Copyright © 2003 John Wiley & Sons, Ltd.

Table II. Relative amounts of product found by multiway SMCR

	Relative amount of product formed	
Batch	Expected	Found by SMCR
I	1.00	1.00
II	1.25	1.28
III	1.25	1.29
IV	0.83	0.73
V	0.83	0.77

The product profile of batch I is in the middle of these five estimates of product profiles. After a sufficiently long time the pair of batches II, III and the pair of batches IV, V reached the same relative concentration. Batch IV was somewhat problematic because of small amounts of baseline drift in the UV/visible spectra, especially at the end of the reaction. A small amount of drift can be seen in the estimated product profile for this batch. Batches II and III had the largest initial charge of reactant, so these two reactions formed more product than the other batches. Moreover, batch III was much faster than batch II owing to the higher reaction temperature. Batches IV and V had the lowest initial charge of reactant, so these two reactions formed the smallest amount of product. Batch V reacted faster than batch IV owing to its higher reaction temperature. Batches II and IV gave smaller initial slopes, indicating that they reacted more slowly compared with batches III and V. These observations are consistent with the expected rates, since batches II and IV were run at 55°C whereas batches III and V were run at 75°C.

3.2. Reaction calorimetry profiles

Figure 6 illustrates the calorimetry profiles of batch I. Three steps were used in the batch process: (1) equilibration, 0–40 min; (2) reagent addition, 40–41 min; (3) run, 41–110 min. Matlab® functions were used to read the WinISO data files and calculate the reaction energy for steps 2 and 3. The calculations were performed using the heat flow calculation method with compensation for small deviations from isothermal operation.

Six steps were involved in the calorimetry calculation method. (1) The reaction power baseline was estimated at the beginning and end of the batch during steady state conditions. During these periods the electrical heat supplied by the heater and controller, Q, is equal to the heat loss to the reactor jacket, reactor lid and instruments immersed in the reaction mixture. (2) Calculation of the heat loss to the jacket was facilitated by the measurement of $\Delta T = T_{\text{reactor}} - T_{\text{jacket}}$ throughout the reaction. The product UA (heat transfer coefficient × wet area) was estimated at the beginning and end of the batch from the measured power baselines and ΔT using Equation (9). (3) Upon addition of the reagent, salicylic acid, the volume of the reaction mixture increased slightly, causing an increase in the wet area A of the reaction mixture in contact with the cold jacket. Since UA changed during reagent addition (~30 s), the slight increase in UA was interpolated over this interval. (4) The heat loss to the jacket was estimated as the product of the interpolated UA profile and measured ΔT profile. It was assumed the rate of heat loss to the lid and instruments remained constant throughout the reaction and is included in step 4. (5) The heater power was compensated by subtracting the estimated heat loss. (6) The resulting compensated heater power was integrated using the trapezoidal rule to give the estimated energy profile.

3.3. Mathematical resolution of calorimetry profiles

In Figure 6 it can be seen that when salicylic acid at room temperature was added to the reactor vessel at 65°C, an initial temperature drop was observed which reflects the amount of heat absorbed as salicylic acid dissolved and warmed from room temperature to the reactor temperature. The exothermic formation of product caused a temperature rise later in the reaction. These two processes, reagent dissolution and product formation, take place at different rates during the batch process and are confounded in the batch energy profiles computed by the method described above. A mathematical fitting method was used to resolve these two different profiles based on the exponential equation

$$Q_t = Q_1(1 - e^{-k_1 t}) + Q_2(1 - e^{-k_2 t}) \qquad (11)$$

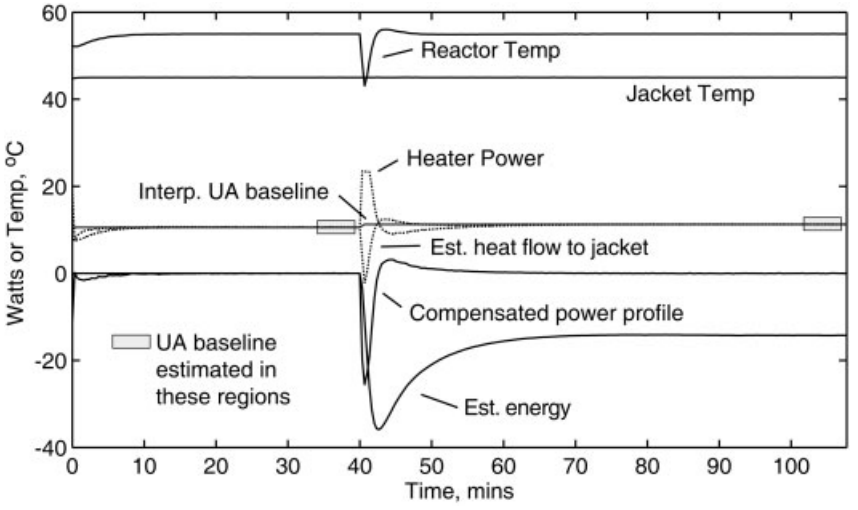

Figure 6. Batch I calorimetry profiles.

Copyright © 2003 John Wiley & Sons, Ltd.

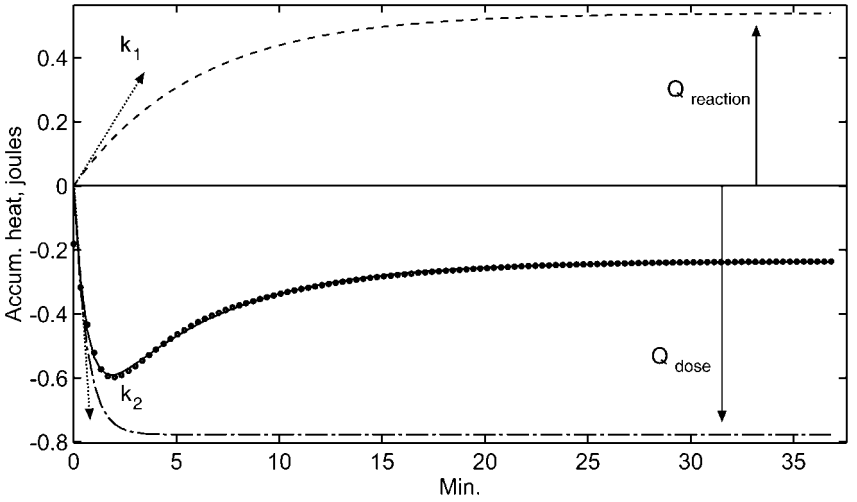

Figure 7. Illustration showing mathematical resolution of the dose heat profile (chain line) and reaction heat profile (broken line) from the measured reaction energy profile (points). Fitted result: full line.

where Q_1 represents the dose heat and includes the heat needed to warm the reactant from room temperature to the reaction temperature plus the reactant dissolution heat and Q_2 represents the heat evolved during the reaction and includes the heat of reaction and the heat of solution of the products. The quantity Q_t is the estimated energy profile shown in Figure 6. It was assumed that the response of the calorimetry system to both processes (dissolution and product formation) followed a pseudo-first-order rate law. The calorimeter response function includes rate constants for these two processes convolved with the calorimeter and heater controller response functions. A Matlab implementation of the quasi-Newton optimization method (fminunc.m) from the Matlab Optimization Toolbox (Version 2) was used to perform the non-linear fitting.

Typical results of the mathematical fitting technique are illustrated in Figure 7. From this non-linear fitting process the rate of dissolution, k_1, can be observed from the initial slope of the dissolution heating curve Q_1, while the rate of reaction, k_2, can be observed from the initial slope of the reaction heating curve Q_2. Residual values from the fitting process were small (in the range of ± 0.002 to ± 0.005 J) and appeared randomly distributed, indicating that the fitted models matched the calorimetry profiles very well.

A summary of the estimated reaction heats and estimated dose heats is shown in Table III. It should be noted that the estimated rate constants k_1 and k_2 obtained from the calorimetry profiles are not reported here because they do not accurately reflect true rate constants owing to time lags in the response of the calorimetry system. Accurate estimates of the reaction rate constants (see Table IV) were obtained by fitting a second-order rate law ($A + B \rightarrow C + D$) directly to the reaction spectra using the method of Bijlsma *et al.* [18]. It was assumed that the reaction mixture was well mixed and that the fiber optic probe response time was very fast compared with the reaction rate. The RMS spectral errors from fitting the second-order rate law to the mixture spectra were small, in the range from 0.002 to 0.007 absorbance units, suggesting that the second-order rate law fitted the spectral data well, even though the reagent, salicylic acid, was introduced manually over a period of about 30–60 s.

To determine the reproducibility of the parameter estimates shown in Tables III and IV, several batches were rerun at 65 and 75°C. The results from repeated runs are shown in

Table IV. Estimated reaction rate constants k from kinetic models fitted to reaction spectra

Experiment	Temp. (°C)	$k(s^{-1})$	RMS error (absorbance units)
I	65	0.023304	0.003802
II	55	0.011721	0.006686
III	75	0.041473	0.002229
IV	55	0.014839	0.005426
V	75	0.048717	0.002497

Table III. Estimated dose heats and reaction heats from calorimetry profiles

Experiment	Temp. (°C)	Mass of SA (g)	Amount of SA (mol)	Est. dose heat (kJ mol^{-1})	Est. reaction heat (kJ mol^{-1})
I	65	8.6806	0.0628	−40.0459	29.6542
II	55	10.8629	0.0786	−34.4872	22.9107
III	75	10.8472	0.0785	−68.2166	55.9774
IV	55	7.2811	0.0527	−34.5452	23.8735
V	75	7.2381	0.0524	−73.7977	58.4785

SA, salicylic acid.

Copyright © 2003 John Wiley & Sons, Ltd.

Table V. Reproducibility of dose heat, reaction heat and reaction rate

Experiment	Temp. (°C)	Mass of SA (g)	Est. dose heat (kJ mol^{-1})	Est. reaction heat (kJ mol^{-1})	Est. reaction rate (mol s^{-1})
I	65	8.6806	−40.05	29.65	0.02330
I	65	8.6967	−40.90	31.06	0.01938
I	65	8.7029	−44.24	33.56	0.01984
Average		8.6934	−41.73	31.42	0.02084
SD		0.0115	2.22	1.98	0.00214
%RSD		0.13%	5.31%	6.30%	10.28%
V	75	7.3001	−73.80	58.48	0.05122
V	75	7.2381	−73.04	57.16	0.04872
Average		7.2691	−73.42	57.82	0.04997
SD		0.0438	0.54	0.93	0.00177
%RSD		0.60%	0.73%	1.61%	3.54%

SA, salicylic acid; SD, standard deviation; RSD, residual standard deviation.

Table V. Compared with the previous runs, the repeated runs of batches I and V demonstrate good reproducibility in the estimated heat of reaction and dose heat. The estimated rate constants, 0.01938 and 0.01984 mols^{-1}, for the replicate trials shown in the second and third rows of Table V are lower than the rate constant shown for the first batch. A long time interval elapsed, ~14 days, between the measurements of these two replicate batches and the first batch. The lower reproducibility between these batches may be attributable to small changes in reagent purity or catalyst concentration over this period of 14 days. The two replicates shown for experiment V in Table VI were run on the same day and showed better reproducibility.

The estimated reaction heats and dose heats are plotted in Figure 8. The heat of reaction is highly temperature-dependent, as is the dose heat, which is an unexpected result. Under constant pressure and volume the heat of reaction is expected to remain constant if the temperature range is narrow. As the reaction temperature is increased, the amount of heat absorbed by the reactant, salicylic acid, is expected to increase; therefore the dose heat is expected to follow a straight line, sloping downward with increasing reaction temperature. As the reaction temperature increased, the experimentally determined heat of reaction increased, while the experimentally determined dose heat decreased.

Some possible explanations for the unexpected curvature in the estimated reaction heat and dose heat are as follows.

1. More than one reaction may take place. The expected product, acetylsalicylic acid, may continue to react with excess acetic anhydride to form acetylsalicylic anhydride. The extent of this secondary reaction may vary at the different conditions employed in these batch reactions, leading to curvature in the plot. A preliminary study of NMR spectra for the products of this reaction suggested that a small amount (~5%) of the doubly acylated acetylsalicylic anhydride was formed.
2. These batches were run at high concentrations under conditions likely to be used in industry, not at infinite dilution where heats of solution approach their limiting values. Because the reaction conditions are far from infinite dilution, the heat of solution can be expected to be strongly dependent on the mass of reactant and temperature, which could be a potential source of curvature observed in Figure 8. Additionally, the reactions were not run at standard conditions, thus the heat of solution for the products, acetylsalicylic acid and acetic acid, are confounded in the heat of reaction reported here.

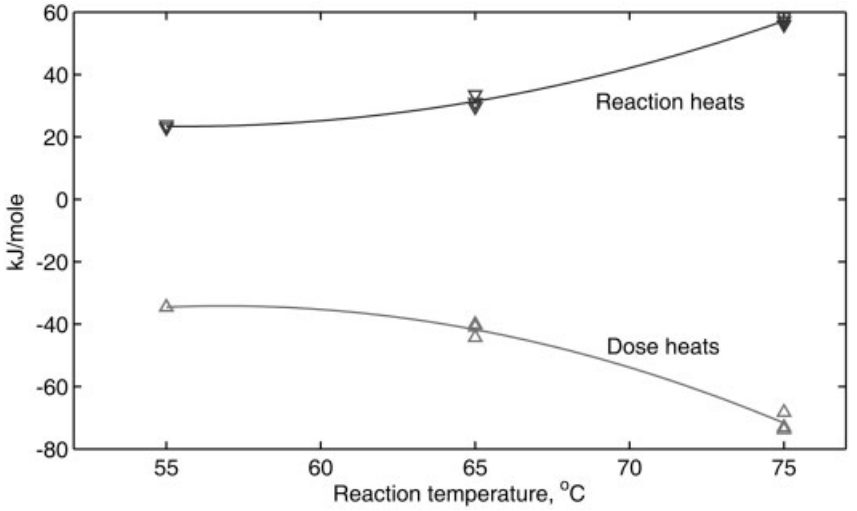

Figure 8. Plot of estimated reaction heats and dose heats.

Copyright © 2003 John Wiley & Sons, Ltd.

4. CONCLUSIONS

In this paper we have demonstrated that it is feasible to thoroughly characterize batch reactions without the aid of reference measurements or standards. *In situ* spectroscopic, calorimetric and temperature measurements were used to develop exploratory models to characterize a series of batch reactions run under different conditions. The chemometric technique of multiway self-modeling curve resolution using non-negative ALS was successfully used to estimate composition profiles. Kinetic models were fitted to reaction calorimetry profiles to give estimates of dose heats and reaction heats. Kinetic models were fitted to *in situ* spectroscopic measurements to estimate rates of reaction.

UV/visible spectroscopy was shown to be a very effective choice for monitoring and characterizing successive batch reactions. Without the aid of reference measurements, two species were observed in the acetylation reaction of salicylic acid with acetic anhydride. Evolving factor analysis was used to automatically and reliably find the location of peaks in multiway SMCR analysis. Multiway SMCR models were used to estimate the relative composition profiles and pure component spectra of different species in the batch. Thus two industrially significant questions were answered. Which reaction produced more or less product? Which reaction produced product faster or slower?

By using the quasi-Newton method of non-linear fitting from the Matlab Optimization Toolbox, kinetic models of calorimetry profiles were constructed. Reaction heat and dissolution heat profiles were mathematically resolved from the measured calorimetry profiles without the use of reference measurements or standards. Repeated measurements demonstrated good reproducibility in the estimated parameters; however, owing to the complexities of the reaction calorimetry conditions, the estimated reaction heats and dissolution heats did not follow expected trends. Rate constants were estimated by fitting kinetic models to *in situ* spectroscopic measurements without the use of standards or reference measurements. Good reproducibility in the estimated rate constants was observed between repeated batches.

Future studies will be aimed at developing techniques that combine *in situ* spectroscopic measurements with calorimetric measurements into one exploratory model.

Acknowledgements

This material is based upon work supported by the National Science Foundation under grant CHE-0201014. The authors wish to recognize the Measurement and Control Engineering Center (MCEC), an NSF University/Industry Cooperative Research Center at the University of Tennessee, for financial support of this project. Also many thanks to our partner, H&A Scientific, Inc. in Greenville, NC, for their technical assistance and development of IntellFORM software.

REFERENCES

1. Friedrich M, Perne R. Design and control of batch reactors—an industrial viewpoint. *Comput. Chem. Eng.* 1995; **19**: S357–S368.
2. Miller CE. Chemometrics for on-line spectroscopy applications—theory and practice. *J. Chemometrics* 2000; **14**: 513–528.
3. Gibson N. Batch process safety. *Chem. Eng.* 1991; **98**: 120–128.
4. Gordon MD. On-line modeling of thermally hazardous batch processes. *Plant/Oper. Prog.* 1992; **11**: 102–105.
5. Quinn AC, Gemperline PJ, Baker B, Zhu M, Walker DS. Fiber-optic UV/visible composition monitoring for process control of batch reactions. *Chemometrics Intell. Lab. Syst.* 1999; **45**: 199–214.
6. Lawton WH, Sylvestre EH. Self modeling curve resolution. *Technometrics* 1971; **13**: 617–633.
7. Gemperline PJ. A priori estimates of the elution profiles of the pure components in overlapped liquid chromatography peaks using target factor analysis. *J. Chem. Info. Comput. Sci.* **1984**; *24*: 206–212.
8. De Juan A, Vander Heyden Y, Tauler R, Massart DL. Assessment of new constraints applied to the alternating least squares method. *Anal. Chim. Acta* 1997; **346**: 307–318.
9. Bro R, Sidiropoulos ND. Least squares algorithms under unimodality and non-negativity constraints. *J. Chemometrics* 1998; **12**: 223–247.
10. Bro R, De Jong S. A fast non-negativity-constrained least squares algorithm. *J. Chemometrics* 1997; **11**: 393–401.
11. Gemperline PJ. Target transformation factor analysis with linear inequality constraints applied to spectroscopic–chromatographic data. *Anal. Chem.* 1986; **58**: 2656–2663.
12. Gampp H, Maeder M, Meyer CJ, Zuberbuhler AD. Calculation of equilibrium constants from multiwavelength spectroscopic data—I. Mathematical considerations. *Talanta* 1985; **32**: 95–101.
13. Tauler R, Kowalski B. Selectivity, local rank, three-way data analysis and ambiguity in multivariate curve resolution. *J. Chemometrics* 1995; **9**: 31–58.
14. Tauler R, Kowalski B, Fleming S. Multivariate curve resolution applied to spectral data from multiple runs of an industrial process. *Anal. Chem.* 1993; **65**: 2040–2047.
15. Duh Y-S, Hsu C-C, Kao C-S, Uy Shuh W. Applications of reaction calorimetry in reaction kinetics and thermal hazard evaluation. *Thermochim. Acta* 1996; **285**: 67–79.
16. Singh J. Reaction calorimetry for process development: recent advances. *Process Saf. Prog.* 1997; **16**: 43–49.
17. Snee TJ, Barcons C, Hernandez H, Zaldivar JM. Characterization of an exothermic reaction using adiabatic and isothermal calorimetry. *J. Thermal Anal.* 1992; **38**: 2729–2747.
18. Bijlsma S, Boelens HFM, Smilde AK. Determination of rate constants in second-order kinetics using UV–visible spectroscopy. *Appl. Spectrosc.* 2001; **55**: 77–83.

Copyright © 2003 John Wiley & Sons, Ltd.